Managing Power Systems-Induced Wildfire Risks Using Optimal Scheduled Shutoffs

Preprint

Ayla Astudillo, Bai Cui, and Ahmed S. Zamzam

National Renewable Energy Laboratory

Presented at the 2022 IEEE Power and Energy Society General Meeting
Denver, Colorado
July 17–21, 2022

NREL is a national laboratory of the U.S. Department of Energy
Office of Energy Efficiency & Renewable Energy
Operated by the Alliance for Sustainable Energy, LLC

This report is available at no cost from the National Renewable Energy Laboratory (NREL) at www.nrel.gov/publications.

Contract No. DE-AC36-08GO28308

Conference Paper
NREL/CP-5D00-81405
July 2022

Managing Power Systems-Induced Wildfire Risks Using Optimal Scheduled Shutoffs

Preprint

Ayla Astudillo, Bai Cui, and Ahmed S. Zamzam

National Renewable Energy Laboratory

Suggested Citation
Astudillo, Ayla, Bai Cui, and Ahmed S. Zamzam. 2022. *Managing Power Systems-Induced Wildfire Risks Using Optimal Scheduled Shutoffs: Preprint*. Golden, CO: National Renewable Energy Laboratory. NREL/CP-5D00-81405. https://www.nrel.gov/docs/fy22osti/81405.pdf.

NREL is a national laboratory of the U.S. Department of Energy
Office of Energy Efficiency & Renewable Energy
Operated by the Alliance for Sustainable Energy, LLC

This report is available at no cost from the National Renewable Energy Laboratory (NREL) at www.nrel.gov/publications.

Contract No. DE-AC36-08GO28308

Conference Paper
NREL/CP-5D00-81405
July 2022

National Renewable Energy Laboratory
15013 Denver West Parkway
Golden, CO 80401
303-275-3000 • www.nrel.gov

NOTICE

This work was authored by the National Renewable Energy Laboratory, operated by Alliance for Sustainable Energy, LLC, for the U.S. Department of Energy (DOE) under Contract No. DE-AC36-08GO28308. The work of A. Astudillo was supported in part by the U.S. Department of Energy, Office of Science, Office of Workforce Development for Teachers and Scientists (WDTS) under the Science Undergraduate Laboratory Internships Program (SULI). The work of B. Cui and A. S. Zamzam was supported by the Laboratory Directed Research and Development (LDRD) Program at NREL. The views expressed herein do not necessarily represent the views of the DOE or the U.S. Government.

This report is available at no cost from the National Renewable Energy Laboratory (NREL) at www.nrel.gov/publications.

U.S. Department of Energy (DOE) reports produced after 1991 and a growing number of pre-1991 documents are available free via www.OSTI.gov.

Cover Photos by Dennis Schroeder: (clockwise, left to right) NREL 51934, NREL 45897, NREL 42160, NREL 45891, NREL 48097, NREL 46526.

NREL prints on paper that contains recycled content.

Managing Power Systems-Induced Wildfire Risks Using Optimal Scheduled Shutoffs

Ayla Astudillo, Bai Cui, and Ahmed S. Zamzam
Power Systems Engineering Center
National Renewable Energy Laboratory
Golden, CO, USA

***Abstract*—The increasing demands for electricity and the increase in extreme weather conditions are putting unprecedented pressure on our electric grids. Often, this pressure leads to electrical component failures, which might ignite wildfires. This work develops a novel model to balance the reliability of power network operations and the risk of wildfire ignition by optimizing the operational schedule of power transmission networks considering time-varying risk measures that include exogenous and operational factors. Energy storage systems are considered to deliver power during peak wildfire hours and enable temporal load shifting. The problem is formulated as a mixed-integer linear program that maximizes a weighted sum of the served power demand and the reduction in grid-induced wildfire risk. The results demonstrate the ability of the model to significantly reduce wildfire risk without considerable load shedding.**

***Index Terms*—wildfires risk management, power systems operations, wildfire-resilient power systems, proactive scheduling**

I. Introduction

Wildfires sparked by electrical components are a rising problem. In 2018, the deadliest wildfire in California's history, the Camp Fire, was caused by faulty transmission lines. Tragically, the town of Paradise was destroyed, 86 people died, and more than $9 billion worth of land was damaged [1]. As a result, Pacific Gas and Electric Company (PG&E) paid more than $13.5 billion in settlement to the victims of the wildfire. Also, the bushfires in the Australian state of Victoria in 2009 were sparked by a faulty component in the electric power infrastructure [2].

Wildfires ignited by failing electric components tend to cause more damage. For example, although wildfires ignited by power lines in San Diego County in California account for only 5% of the wildfires there, they account for more than 25% of all losses from wildfires [3]. This is mainly because of the commonality of the factors that cause faults in electric power systems and the circumstances that aggravate wildfires, such as hot, dry, and windy weather [4].

As a preventative measure, electric system operators often resort to power shutoffs to reduce the probability of igniting a wildfire [5]; however, such strategies harm end users that lose access to electricity for long periods, especially during heat waves. This harm can be further exacerbated for vulnerable and overburdened communities [6]. Other detection methods and monitoring and surveillance techniques, as highlighted in [7], aim to manage wildfire ignition risk and limit the damage caused by them. In [8], ways that wildfires and their subsequent impact can be mitigated are presented including preventing faults and ignitions and strategies to limit the impacts of wildfires if an power system-induced ignition occurs. An additional solution to eliminate ignitions from electric grids is to convert overhead transmission lines to underground cables, but this is costly and time extensive. A recent approach proposed an optimization model to identify line upgrades that are optimal in terms of mitigating wildfire risk [9].

To provide more efficient management of wildfire risk, an optimal shutoff problem was formulated in [10] where the grid operations are optimized to balance the power shutoffs and the wildfire ignition risk. The proposed model selectively de-energizes transmission lines and grid components to mitigate their associated wildfire risks while limiting power shutoffs. The proposed approach considers a short-term operational time frame that can be represented as a single time step; however, because the duration of high wildfire risk often spans multiple hours, it is necessary to plan the operation of power systems throughout such periods considering varying grid and environment conditions.

This paper proposes an optimal scheduling framework for managing power system-induced wildfire risk. We introduce multiple time steps so that the risk of wildfire and load delivery fluctuate with changes in temperature and power demand throughout the day. In addition to accounting for critical ramping constraints, the proposed optimization model allows for temporal considerations for both power delivery and wildfire risk. In particular, the main advantages of this framework are: 1) coupling the component risk values with

This work was authored by the National Renewable Energy Laboratory (NREL), operated by Alliance for Sustainable Energy, LLC, for the U.S. Department of Energy (DOE) under Contract No. DE-AC36-08GO28308. The work of A. Astudillo was supported in part by the U.S. Department of Energy, Office of Science, Office of Workforce Development for Teachers and Scientists (WDTS) under the Science Undergraduate Laboratory Internships Program (SULI). The work of B. Cui and A. S. Zamzam was supported by the Laboratory Directed Research and Development (LDRD) Program at NREL. The views expressed in the article do not necessarily represent the views of the DOE or the U.S. Government. The U.S. Government retains and the publisher, by accepting the article for publication, acknowledges that the U.S. Government retains a nonexclusive, paid-up, irrevocable, worldwide license to publish or reproduce the published form of this work, or allow others to do so, for U.S. Government purposes. Emails: ayla.m.astudillo@gmail.com, {bai.cui, ahmed.zamzam}@nrel.gov

external factors, such as ambient temperature and operational settings, such as power flow in lines, because the intensity of the sparks in faulty lines are proportional to the energy flowing through the line prior to the fault; and 2) modeling temporal operational constraints and the incorporation of energy storage units that can shift loads temporally to minimize wildfire risk on grid components during high-risk periods. As a result, our model can identify scheduled decisions to de-energize electrical components and redirect power flow on an hourly basis. The efficacy of the proposed model is demonstrated on a version of the RTS-GMLC test case [11], located in Southern California, augmented with temprature data from these regions as well as component risk information. The proposed framework is shown to provide significant reduction in wildfire risk while limiting power shutoffs during the considered day of operation.

II. Background

A. Power Systems Modeling

We consider a connected and phase-balanced power system in steady state. The underlying topology of the system can be described by an undirected connected graph, $\mathcal{G} = (\mathcal{B}, \mathcal{E})$, where buses are modeled as vertices, $\mathcal{B}$, and lines are represented by edges $\mathcal{E} \subseteq \mathcal{B} \times \mathcal{B}$. Three types of system components can be connected to a bus: a load, an energy storage unit, and one or more generators. Let $\mathcal{G}$ be the set of generators, and $\mathcal{G}(i) \subseteq \mathcal{G}$ be the set of generators at bus i. $\mathcal{G}(i) = \varnothing$ if there are no generators at bus i. We assume a bus can have at most one energy storage unit, and we index them by the corresponding bus numbers. We denote the set of energy storage units by $\mathcal{Q} \subseteq \mathcal{B}$. Similarly, we index a load using the bus it is located at and let $\bar{P}_i^D \geq 0$ be the rated power demand of the load. The demand, $\bar{P}_i^D$, is set to zero when no load is present at bus $i \in \mathcal{B}$.

The power from a generator is limited by:

$$\underline{P}_i^G \leq P_i^G \leq \bar{P}_i^G, \qquad \forall i \in \mathcal{G}. \tag{1}$$

Because a generator is allowed to turn on/off, we extend this equation to:

$$z_i^G \underline{P}_i^G \leq P_i^G \leq z_i^G \bar{P}_i^G, \qquad \forall i \in \mathcal{G}. \tag{2}$$

where the binary variable, z_i^G, is the energization indicator for generator $i \in \mathcal{G}$. Generator i is on if $z_i^G = 1$ and off if $z_i^G = 0$. If the generator is off, then the equation enforces $P_i^G = 0$ for the generator.

Similarly, the actual power consumption from a load is constrained by:

$$0 \leq P_i^D \leq z_i^D \bar{P}_i^D, \qquad i \in \mathcal{B}, \tag{3}$$

where the binary z_i^D is the energization indicator for the load at bus $i \in \mathcal{B}$.

The DC power flow model is used in the paper. For every bus $i \in \mathcal{B}$, the following voltage phase angle constraints are imposed:

$$\underline{\theta}_i \leq \theta_i \leq \bar{\theta}_i. \tag{4}$$

The phase angle of the slack bus, $s \in \mathcal{B}$, is fixed at zero, so:

$$\underline{\theta}_s = \bar{\theta}_s = 0. \tag{5}$$

Every transmission line, $\ell \in \mathcal{E}$, has power limit $\bar{f}_\ell$, so the line flow, f_ℓ, is constrained as:

$$-\bar{f}_\ell \leq f_\ell \leq \bar{f}_\ell, \qquad \forall \ell \in \mathcal{E}. \tag{6}$$

This equation can be similarly extended to incorporate line energization as:

$$-z_\ell^L \bar{f}_\ell \leq f_\ell \leq z_\ell^L \bar{f}_\ell, \qquad \forall \ell \in \mathcal{E}, \tag{7}$$

where the binary variable $z_\ell^L = 0$ when line $\ell \in \mathcal{E}$ is open, and $z_\ell^L = 1$ when it is closed.

Let $\mathbf{B} \in \mathbb{R}^{|\mathcal{E}| \times |\mathcal{E}|}$ be the diagonal matrix with line susceptance on the diagonal, and let $\mathbf{A} \in \mathbb{R}^{|\mathcal{B}| \times |\mathcal{E}|}$ be the node-edge incidence matrix, such that:

$$A_{i\ell} = \begin{cases} 1, & \text{if } \ell = (i,j) \text{ for some } j, \\ -1, & \text{if } \ell = (j,i) \text{ for some } j, \\ 0, & \text{otherwise.} \end{cases} \tag{8}$$

Based on the DC power flow model, we have:

$$\mathbf{f} = \mathbf{B}\mathbf{A}^\top \boldsymbol{\theta}. \tag{9}$$

The equation can be extended to incorporate the line energization through big-M notation as:

$$\mathbf{f} - M(\mathbb{1} - \mathbf{z}^L) \leq \mathbf{B}\mathbf{A}^\top \boldsymbol{\theta} \leq \mathbf{f} + M(\mathbb{1} - \mathbf{z}^L), \tag{10}$$

where $M > 0$ is a sufficiently large number. A single M is used in (10) for the sake of exposition, but different M can be used for different constraints to improve the computational performance.

The node power balance equation is:

$$\mathbf{P} = \mathbf{A}\mathbf{f}, \tag{11}$$

where the net power injection, $\mathbf{P}$, is:

$$P_i = -P_i^D - P_i^E + \sum_{j \in \mathcal{G}(i)} P_j^G, \qquad \forall i \in \mathcal{B}, \tag{12}$$

where P_i^E is the energy storage unit charging power at bus i. When the bus has no energy storage unit, the corresponding value is set to zero.

To limit the number of switching decisions for the amount of generators and transmission lines, the following constraints are imposed:

$$\sum_{i \in \mathcal{G}} (1 - z_i^G) \leq \bar{G}, \tag{13}$$

and:

$$\sum_{\ell \in \mathcal{E}} (1 - z_\ell^L) \leq \bar{L}, \tag{14}$$

where $\bar{G}$ and $\bar{L}$ are the maximum number of switching decisions for the generators and the transmission lines. If a bus is de-energnized, then the connecting loads, generators,

and adjacent lines must be de-energized too. This is enforced by the following connectivity constraints:

$$z_i \geq z_i^D, \quad \forall i \in \mathcal{B}, \tag{15a}$$
$$z_i \geq z_j^G, \quad \forall i \in \mathcal{B}, j \in \mathcal{G}(i), \tag{15b}$$
$$z_i \geq z_\ell^L, \quad \forall i \in \mathcal{B}, \ell = (i,j) \text{ or } (j,i) \text{ and } \ell \in \mathcal{E}, \tag{15c}$$

where the binary variable, z_i, is the energization indicator for bus $i \in \mathcal{B}$.

In case there are multiple time steps, constraints (4)–(15) are imposed for all the steps. The set of time steps is denoted by $\mathcal{T} := \{1, 2, \ldots, T\}$.

B. Ramping Limits

When we extend the problem formulation to include time steps, it is important to consider ramping limits for generators, load shedding, and energy storage units. Because we have multiple time steps where we change the power output to optimize the power system while reducing the wildfire risk, we want constraints that limit the change in power from one time step to the next.

Let r_i^G be the ramping limit for generator $i \in \mathcal{G}$, then the ramping constraints for the generator are expressed by:

$$-r_i^G \leq P_{i,t}^G - P_{i,t-1}^G \leq r_i^G, \qquad \forall i \in \mathcal{G}, t \in \mathcal{T}. \tag{16}$$

where the initial generation profile, $P_{i,0}^G$, is given.

Similarly, the ramping constraints for the load is given by:

$$-r_i^D \leq P_{i,t}^D - P_{i,t-1}^D \leq r_i^D, \qquad \forall i \in \mathcal{B}, t \in \mathcal{T}, \tag{17}$$

where r_i^D is the ramping limit for the load at bus $i \in \mathcal{B}$, and $P_{i,0}^D := \bar{P}_i^D$ is the full power demand. Constraint (17) limits the ramp rate of the load shedding.

C. Energy Storage Units

The initial state of charge, $S_{i,0}$, is given for all energy storage units, $i \in \mathcal{Q}$. We assume that the state of charge at the end of the time horizon should be no less than the initial one, so the following constraints are imposed:

$$S_{i,T} \geq S_{i,0}, \qquad \forall i \in \mathcal{Q} \tag{18}$$

The energy storage unit, $i \in \mathcal{Q}$, acts as a load when it is charging ($P_i^E \geq 0$), and it acts as a generator when it is discharging ($P_i^E \leq 0$). The charging and discharging rate for the battery is limited by:

$$\underline{P}_i^E \leq P_i^E \leq \bar{P}_i^E, \qquad \forall i \in \mathcal{Q}, t \in \mathcal{T}. \tag{19}$$

where $\underline{P}_i^E$ is the maximum discharging rate, and $\bar{P}_i^E$ is the maximum charging rate. We calculate the current state of charge with:

$$S_{i,t} = S_{i,t-1} + P_{i,t-1}^E \Delta t \qquad \forall i \in \mathcal{Q}, t \in \mathcal{T}, \tag{20}$$

where Δt is the duration of one time step.

III. Optimization Formulation for Optimal Power Shutoffs

We introduce the multiperiod optimal power shutoff (M-OPS) problem formulation in this section. The problem tries to determine the optimal power dispatch and component shutoffs operations to mitigate wildfire risk while maintaining a certain level of power reliability (measured by the amount of load shedding). The risk mitigation is achieved by not only the optimal scheduling of the component shutoffs but also the power flow rerouting on heavily loaded lines. This will become clearer when the objective function is introduced.

In the objective function of the M-OPS, $\alpha \in [0,1]$ is a parameter that controls the weight of the wildfire risk and the willingness to perform load shedding. A system operator would choose an α to determine the trade-off between delivering power and reducing wildfire risk for the system. The two competing objectives are denoted by D_{total} and R_{fire}, respectively, where:

$$D_{\text{total}} = \sum_{t \in \mathcal{T}} \sum_{i \in \mathcal{B}} x_{i,t} P_{i,t}^D \tag{21}$$

is the total load served across the entire scheduling horizon, and:

$$R_{\text{fire}} = \sum_{t \in \mathcal{T}} \Big(\sum_{i \in \mathcal{B}} R_{i,t}^D \frac{P_{i,t}^D}{\bar{P}_i^D} + \sum_{i \in \mathcal{L}} R_{\ell,t}^L \frac{|f_{\ell,t}|}{\bar{f}_\ell} + \sum_{i \in \mathcal{G}} R_{i,t}^G z_{i,t}^G + \sum_{i \in \mathcal{G}} R_{i,t}^B z_{i,t} \Big) \tag{22}$$

is the aggregated multiperiod wildfire risk. The parameters $R_{i,t}^D, R_{i,t}^G, R_{i,t}^B$, and $R_{i,t}^L$ are the given risk values for loads, generators, buses, and transmission lines at time t. Note that the risks associated with the buses and generators are binary: they are either the specified risk values when the component is on, or zero otherwise. On the other hand, the transmission line and load risks scale with the power, signifying the proportionality between the wildfire risk and the loading condition.

With the risk and power delivery metrics in place, the M-OPS problem can be formulated as follows:

$$\max \quad (1-\alpha) D_{\text{total}} - \alpha R_{\text{fire}} \tag{23a}$$
$$\text{s.t} \quad (4), (5), (2), (7), \quad \text{(operational constraints)} \tag{23b}$$
$$(10)\text{–}(12), \quad \text{(power flow constraints)} \tag{23c}$$
$$(13)\text{–}(14), \quad \text{(switching constrains)} \tag{23d}$$
$$(15), \quad \text{(connectivity constraints)} \tag{23e}$$
$$(16)\text{–}(17), \quad \text{(ramping limits)} \tag{23f}$$
$$(18)\text{–}(20), \quad \text{(energy storage constraints)} \tag{23g}$$

One should be careful when setting α to 0 or 1 in this problem. When $\alpha = 1$, the optimal solution will gradually turn the entire system off to the point of a complete blackout, the process of which is constrained only by the ramping limits. This is obviously not an acceptable operation strategy. On the other hand, when $\alpha = 0$, the optimization problem resembles a multiperiod OPF problem with no objective function where

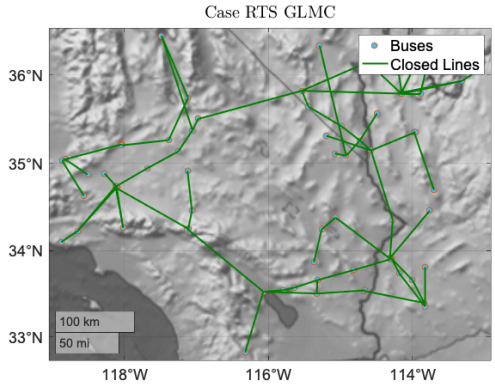

Fig. 1: Map of the RTS-GMLC network. Red dots represent buses with energy storage systems installed.

the loads are fixed at their rated values, but it is still preferred that the solution would be the one with the lowest risk value, R_{fire}, under full load condition. In summary, we prefer the optimal solutions in both scenarios to be those that optimize the secondary objective (either D_{total} or R_{fire}) among those that optimize the primary one. Thanks to the discrete nature of the problem, this might be achieved by setting α to δ or $1-\delta$ instead of 0 or 1, where δ is a very small number. This is empirically supported in our numerical studies.

IV. Test Case and Numerical Simulations

A. Network Specifications

We test our model using the RTS-GMLC test network [11]. The test case represents a power system that is assumed to be located in Southern California and parts of Nevada and Arizona. The network consists of 73 buses, 120 lines, and 96 active generators. The transmission lines in the system are shown in green in Fig. 1 on a map of the southwest of the United States. For our tests, we assume that there are no upper bounds on the number of transmission lines and generators that can be switched off, i.e., $\bar{L} = \bar{G} = \infty$.

B. Risk Values

In this work, we use the risk values for the buses, $\mathbf{R}^B$, and transmission lines, $\mathbf{R}^L$, obtained from the source code of [10]. The authors of [10] proposed a wildfire risk map that relates risk to location in a realistic setting. The wildfire risk levels are low in regions with no history of wildfires, and the risk values are at their extreme for regions with repeated wildfires disasters. For simplicity, it is assumed that buses with low risk are assigned $R^B = 0$, whereas buses with medium, high, and extreme wildfire risk are assigned $R^B = 1$, $R^B = 2$, and $R^B = 4$, respectively. The line risk is computed by calculating the risk of each section depending on the region where the sections are located. We also assume that the risk values of generators and the load are the same as the bus they are connected to, i.e., $R_j^G = R_i^D = R_i^B$, whenever the generator j is located at bus i, i.e., $j \in \mathcal{G}(i)$.

This results in a single risk value for each component in the system. To vary the risk values with varying exogenous conditions, we relate the risk values with the ambient temperature as follows. First, we separate the electrical components by area. Notice in Fig. 1 that the system naturally clusters into three areas. Weather data were collected from weather stations located within each area. Temperature time series were obtained for the three areas for 24 hours on July 4, 2020, in Palm Springs, CA, Bullhead, AZ, and Burbank, CA (areas 1, 2, and 3, respectively). July 4 represents a summer day with noticeable temperature fluctuations throughout the day. The risk values of the electrical components are scaled according to the temperature in the corresponding region where the component is located. Consequently, instead of having a single risk value for each component, we obtain time-varying risk values for different time steps, $t \in \mathcal{T}$.

For the transmission lines, scaling the risk to temperature is slightly different when the lines cross areas. Instead of scaling according to a single temperature time series, the average of the two time series is used to scale the risk values of the lines.

C. Power Demand

Similar to scaling the risk to temperature, the power demands, $\bar{\mathbf{P}}^D$, are scaled using historical power consumption data. We collect real data on power consumption from three electrical companies: PG&E, Southern California Edison, and San Diego Gas and Electric Company [12]. We associate each utility data with an area in the network. Then, the baseload values are scaled according to the time series of the load demands in the corresponding region such that the average power demand during the day is the single power demand value that is given in the network specifications.

D. Energy Storage Units

TABLE I: Ratings of Energy Storage Units

Bus No.	Capacity	Max Charge Rate	Max Discharge Rate
114	350	50	−50
116	450	50	−50
207	400	50	−50
221	300	45	−45
301	400	40	−40
313	550	60	−60

To facilitate load-shifting behavior, a total of six utility-scale energy storage systems [13] are assumed to be installed in the network. Table I presents the specifications of the energy storage units along with the buses where they are connected. There are two energy storage units in each area to assist in case sections of the grid are disconnected from the rest of the network. The locations of the energy storage systems are depicted in red in Fig. 1. If fully charged, these energy storage systems can provide at least 6 hours of energy at approximately 50 MW per hour. It is expected that the proposed model will result in drawing energy from storage systems during peak wildfire hours due to high risks from an increase in temperature.

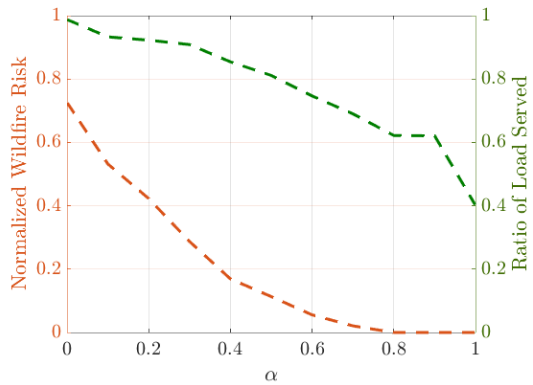

Fig. 2: The wildfire risk and demand served with varying α in M-OPS

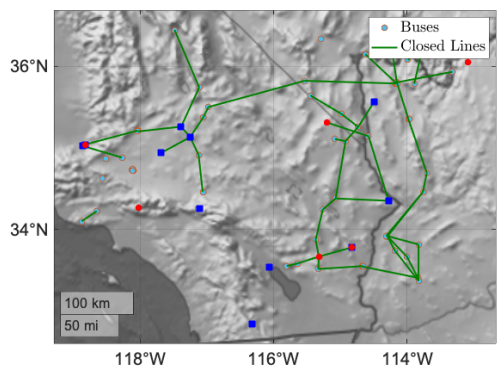

Fig. 3: Map of the operational system when $\alpha = 0.3$ at 12:00 PM. Blue squares represent shutoff generators.

E. Numerical Results

First, we assess the performance of the proposed problem formulation. The value of α that controls the tendency of the approach to favor either the amount of loads served or the reduction in wildfire risk is varied between 0 and 1. To avoid ill-posed formulations, we use 10^{-3} and $1-10^{-3}$ to substitute the tests with α value equal to 0 and 1, respectively. We compute the risk value associated with operating the network while minimizing the total generation cost. Then, we use this risk value to normalize the risk associated with any operational trajectory. We implemented the proposed formulation using MATLAB and utilizing CPLEX as a mixed-integer linear programming solver [14].

Fig. 2 depicts the reduction in load served as well the reduction in wildfire risk associated with increasing the value of α. Notice that as α increases, the demand decreases but at a much slower rate than the risk of wildfires. This demonstrates the efficacy of the proposed approach in identifying solutions that significantly reduce the wildfire risk without considerable load shedding. Specifically, the wildfire risk can be reduced to less than 20% of the original risk while serving more than 80% of the loads in the network.

The map in Fig. 3 shows the solution to M-OPS when the system is operating at 90% when $\alpha = 0.3$ at noon on July 4, 2020. There are 31 generators switched off and 62 open transmission lines. The generators that are turned off are depicted as blue squares in Fig. 3. The lines that remain on have individual wildfire risk values of zero or near zero, which explains how the systems reduces wildfire risk while serving almost 90% of the load.

V. Concluding Remarks

In this paper, a model was developed to manage the risk of wildfires induced by failing electrical components with an optimal power shutoff scheduling. The model accounts for time-varying risk measures by considering exogenous factors, such as temperature, and intrinsic factors, such as power flow in lines. The model also incorporates energy storage systems that can help alleviate wildfire risks by temporally shifting power demand. The results show that the proposed model can identify operational schedules that mitigate wildfire risk from an existing power network while serving 98%–62% of the power demand.

Future work may include N-1 contingencies that are important to reliably operate the system in the event of a single failure. In addition, the development of decomposition and relaxation approaches can provide scalable solutions that enable applying the proposed formulation to larger networks.

References

[1] "Camp fire: By the numbers." [Online]. Available: https://www.pbs.org/wgbh/frontline/article/camp-fire-by-the-numbers/

[2] The Victorian Bushfires Royal Commission, "The final report of the 2009 Victorian bushfires," July 2010. [Online]. Available: http://royalcommission.vic.gov.au/Commission-Reports/Final-Report.html

[3] A. D. Syphard and J. E. Keeley, "Location, timing and extent of wildfire vary by cause of ignition," *International Journal of Wildland Fire*, vol. 24, no. 1, pp. 37–47, 2015.

[4] C. Miller, M. Plucinski, A. Sullivan, A. Stephenson, C. Huston, K. Charman, M. Prakash, and S. Dunstall, "Electrically caused wildfires in Victoria, Australia are over-represented when fire danger is elevated," *Landscape and Urban Planning*, vol. 167, pp. 267–274, 2017.

[5] Pacific Gas & Electric Company, "Public safety power shutoff policies and procedures," August 2021.

[6] M. Sotolongo, C. Bolon, and S. Baker, "California power shut-offs: Deficiencies in data and reporting," *Initiative for Energy Justice*, 2020.

[7] S. Jazebi, F. De Leon, and A. Nelson, "Review of wildfire management techniques—Part I: Causes, prevention, detection, suppression, and data analytics," *IEEE Trans. Power Del.*, vol. 35, no. 1, pp. 430–439, 2019.

[8] J. W. Muhs, M. Parvania, and M. Shahidehpour, "Wildfire risk mitigation: A paradigm shift in power systems planning and operation," *IEEE Open Access Journal of Power and Energy*, vol. 7, pp. 366–375, 2020.

[9] S. Taylor and L. A. Roald. (2021) A framework for risk assessment and optimal line upgrade selection to mitigate wildfire risk. [Online]. Available: https://arxiv.org/abs/2110.07348

[10] N. Rhodes, L. Ntaimo, and L. Roald, "Balancing wildfire risk and power outages through optimized power shut-offs," *IEEE Trans. Power Syst.*, vol. 36, no. 4, pp. 3118–3128, 2021.

[11] C. Barrows, A. Bloom, A. Ehlen, J. Ikäheimo, J. Jorgenson, D. Krishnamurthy, J. Lau, B. McBennett, M. O'Connell, E. Preston, A. Staid, G. Stephen, and J.-P. Watson, "The ieee reliability test system: A proposed 2019 update," *IEEE Trans. Power Syst.*, vol. 35, no. 1, pp. 119–127, 2020.

[12] California Independent System Operator, "Historical hourly load data from EMS," August 2020. [Online]. Available: http://www.caiso.com/planning/Pages/ReliabilityRequirements/Default.aspx#Historical

[13] R. Carnegie, D. Gotham, D. Nderitu, and P. V. Preckel, "Utility scale energy storage systems," *State Utility Forecasting Group. Purdue University*, vol. 1, 2013.

[14] CPLEX, IBM ILOG, "V12.1: User's Manual for CPLEX," *International Business Machines Corporation*, vol. 46, no. 53, p. 157, 2009.